Sp5 Stimulation leads to Prolonged Excitation in AVCN and Inhibition in DCN neurons

Senior Honors Thesis

Shashwati Pradhan

4/1/2010

Abstract

In addition to receiving inputs from the auditory nerve, the guinea pig cochlear nucleus (CN) also receives inputs from the somatosensory system (Shore et. al., 2000; Zhou and Shore, 2004). While most of these inputs terminate in the granule cell domain (GCD) of the CN, the magnocellular regions of antero-ventral cochlear nucleus (AVCN) and dorsal cochlear nucleus (DCN) also receive excitatory (glutamatergic) inputs from the spinal trigeminal nucleus (Sp5; Zhou and Shore, 2004; Zhou et. al., 2007), a region associated with somatosensation from the vocal tract/intra oral structures and face (Romfh et al., 1979; Capra, 1987; Jacquin et al., 1989; Nazruddin et al., 1989; Takemura et al., 1991; Suemune et al., 1992).

Previous studies have investigated the short-term modulation of firing properties of CN neurons by electrical stimulation of the trigeminal system (Shore et. al. 2003; Shore, 2005; Shore et. al., 2008). However, in this study, we examine the long-term effects of bimodal (acoustic and somatosensory) stimulation on the firing rate of neurons in the AVCN and DCN. Unit responses were recorded using multi-channel electrodes placed into the DCN and VCN of ketamine-anesthetized guinea pigs. Rate-level functions (RLFs), obtained at characteristic frequency (CF), were used to determine changes in the sound-driven firing rates of units by bimodal stimulation. RLFs were measured for several minutes before and after bimodal stimulation. The current stimulus consisted of two biphasic pulses with 60 μA and 100 μs/phase. Primary-like and Primary-like with Notch AVCN units showed a prolonged, significant increase in firing rate after bimodal stimulation. In contrast, units in the DCN showed a long lasting decrease in firing rate.

Introduction

The cochlear nucleus (CN) contains the second-order neurons of the auditory brainstem and plays an important part in the processing of auditory inputs provided by the VIIIth Cranial Nerve, which is also known as the auditory nerve. The fibers of the auditory nerve branch, providing inputs to the three distinct regions of the CN: the dorsal CN (DCN), antero-ventral CN (AVCN) and postero-ventral CN (PVCN; Hackney et. al., 1990). Each region contains a unique set of cells that, after initial processing, send axons to higher auditory centers such as the trapezoid body, the superior olivary complex and the inferior colliculus (Hackney et. al., 1990; Oertel & Young, 2004).

However, studies have shown that the CN receives not only auditory input, but also somatosensory innervation originating in the trigeminal ganglion, the spinal trigeminal nucleus of the Vth Cranial Nerve (Sp5) and the cuneate nucleus (Weinberg & Rustoni, 1987; Wright & Ryugo, 1996; Shore et. al., 2003, Zhou & Shore, 2004). These somatosensory projections have been hypothesized to play a part in sound localization and suppress self-generated sounds (Kanold and Young, 2001; Bell et al., 1997; Shore, 2005; Zhou et. al., 2007). Sp5, the somatosensory nucleus of focus in this study, conveys information pertaining to head/neck position and vocalization (Kirzinger & Jurgens, 1991; Luthe et. al., 2000). Excitatory projections from Sp5 (Zhou et al., 2007) terminate primarily in the CN granule cell domain (GCD), which is situated over the medial, dorsal, and lateral surface of the VCN and expands into layer II of the DCN and contains mainly granule cells that participate in the local circuit with DCN (Ryugo et. al., 2003). Excitatory inputs from the granule cells via their unmyelinated axons (the

3

parallel fibers) terminate on the apical dendrites of pyramidal cells, the principal output neurons of DCN, which also receive auditory inputs on their basal dendrites, mimicking cerebellar circuitry (Oertel and Young, 2004; Figure 1). The parallel fibers also terminate on inhibitory interneurons, the cartwheel cells, which terminate on pyramidal cells (Oertel and Young, 2004). Somatosensory stimulation in the DCN can suppress or enhance response rates to subsequent acoustic stimuli and may also alter spike timing (Shore, 2005; Shore et. al., 2008). These results have shown that pyramidal cells play an important role in multisensory integration stimulating studies on multisensory integration in the CN that exclusively focused on the DCN.

However, studies also point towards a possible role of the AVCN in multisensory integration. Anatomical tracer studies have shown that, in addition to projecting to the GCD, Sp5 projects to the magnocellular regions of AVCN (Zhou and Shore, 2004). Immunocytochemical studies further elucidated that, like projections to the GCD, somatosensory projections to AVCN are also excitatory and use glutamate as a neurotransmitter (Zhou et. al., 2007). It is most likely that Spherical Bushy Cells (SBCs) and Globular Bushy Cells (GBCs) – major cells present in the magnocellular core of the AVCN (Hackney et. al., 1990) – receive these somatosensory inputs from Sp5 (Shore et al., 2003). Bushy cells project to the trapezoid body and superior olivary complex and are origin of pathways involved in the processing of interaural time and level differences (Hackney et. al. 1990, review: Cant and Benson, 2003). The existence of somatosensory projections to AVCN suggests that perhaps it is also an important site of multisensory integration.

Methods

Surgical Preparation

Experiments were performed on 4 adult, male, pigmented guinea pigs (350-600 g, Elm Hill). All procedures were approved by the University of Michigan Committee on the Use and Care of Animals. Animals were anesthetized with ketamine (120 mg/kg) and xylazine (6 mg/kg, IM) and held in a stereotaxic device (David Kopf Instruments, Tujunga, California) with hollow ear bars for sound delivery. Rectal temperature was monitored and maintained at 38 $\pm$ 0.5°C with a thermostatically controlled heating pad. Supplemental anesthesia (0.2 ml of 16mg ketamine and 0.8mg xylazine) was given approximately hourly, after performing a pinch test to elicit paw withdrawal. Core temperature, pulse rate and blood oxygen level were monitored throughout the experiment to ensure that the condition of the animal was stable. A craniotomy and partial aspiration of the cerebellum overlying the DCN was performed to allow the visual placement of the stimulating and recording probes in the Sp5 and CN.

Sp5 Stimulation

Sp5 neurons were activated by passing current through a bipolar concentric stimulating electrode (Frederick Haer and Co., Bowdoin, ME) directed towards the Sp5 interpolaris (Sp5i) or the Sp5 caudalis (Sp5c) – regions of the Sp5 from where projections to CN were previously observed – using stereotaxic coordinates (0.30 cm lateral from midline, 0.22 cm caudal to the transverse sinus, 0.95 cm below surface of cerebellum; Zhou and Shore, 2004). Two biphasic pulses (100 µs/phase, negative phase first) with a pulse frequency of 1000Hz and varying amplitudes (40-60uA) were used as the current

stimulus, that preceded the tone stimulation by 20ms. In all experiments, the stimulating electrode was dipped in Fluoro-Gold before insertion to enable post mortem reconstruction of the electrode positions (see Histology below).

Acoustic Stimulation

Acoustic stimuli were presented at different sound pressure levels to assess thresholds, characteristic frequencies (CFs), latencies and rate-level functions (RLFs). Stimuli were delivered with Beyer dynamic earphones (DT-770 pro) coupled to hollow ear bars. TDT system III hardware (Tucker-Davis Technology, Alachua, FL) was used for digital-to-analog conversion and analog attenuation. Digital signals were generated by a PC (Intel Core2 Duo) using a custom TDT OpenEx software package. Stimuli were generated using a sampling rate of 50 kHz with 16-bit resolution. Tones were calibrated using a ¼ inch condenser microphone (Bruel & Kjaer, Mic:4136, Preamp:2619, Power Supply:2804). The microphone output was measured using custom OpenEx software. Noise was calibrated with the ¼ inch microphone and coupler attached to a sound level meter set to measure the bandwidth of interest (200 Hz-20 kHz for BBN). Equalization to correct for the system response was performed in the frequency domain using digital filters implemented in TDT hardware. The stimulus variable sequences were generated from within OpenEx. The maximum output of the system was 85 db SPL between 0.1 kHz and 36kHz. For recordings conducted with bimodal stimulation, Sp5 stimulation preceded the acoustic stimulus by 20 ms for each repetition.

Data Acquisition

Recordings were made in a sound-attenuating double-walled booth (ETS Lindergren Acoustic Systems). A single-shank, 16-channel silicon substrate electrode (177μm^2 sites, Neuronexus Inc, Michigan) was used to record activity from many units simultaneously (Figure 2A). For insertion into the AVCN, the electrode was inclined to an angle of 30° from vertical. The probe was visually positioned using the paraflocular recess as an anatomical marker and the probe tip was inserted rostral to this structure. It was advanced 2-3 mm below the surface of the DCN in a ventro-rostral direction. If necessary, the electrode was repositioned until robust responses to ipsilateral acoustic stimulation were obtained.

The 16-channel electrode was connected by a 16-channel pre-amplifier and digitizer to a TDT data-acquisition system. The signals were filtered from 300–7500 Hz prior to analog-to-digital conversion. Analog-to-digital conversion was performed by simultaneous-sampling 12-bit converters at 25 kHz per channel. A spike detection threshold was set independently for each recording channel to 1.2 SDs above the mean background noise voltage. Timestamps and associated waveforms were recorded at each threshold crossing.

Threshold and characteristic frequencies were determined from a receptive field generated from responses to 10 repetitions of a 50ms duration tone (5ms ramps) at each frequency-level condition (resolution 0.1 octave and 5dB steps). Post-stimulus Time Histograms (PSTHs) were recorded for 300 repetitions (50ms tone duration,

200ms stimulation period) at the unit's CF and several sound levels for assessment of unit response type. Firing rates at CF were recorded using the following stimulus paradigm: First 4 RLFs were conducted ascending levels of pure tone stimulation followed by a single bimodal (acoustic and Sp5 stimulation) RLF. Finally, 4 RLFs were repeated with intervals of 10 minutes per RLF.

Spike sorting

Spike waveforms were sorted using TDT OpenSorter software package. The time period of the electrical artifact was excluded before sorting. Principal component analysis was conducted by OpenSorter and used to generate J2 statistics, which measure separation of cluster pairs. Four passes of custom MATLAB software were done to automatically combine pairs of cluster with a J2 below 10^{-5} assuming that a J2 above 10^{-5} characterizes separate clusters. Clusters were then manually judged to be single or multiunit based on the results of principle component analysis. Multiunit classification signifies that multiple neurons contributed to the firing rates recorded.

Data analysis

Data analysis was performed using OpenExplorer software (TDT), Sigmaplot (v11 for Windows, Systat Software, Germany) and SPSS (v17, SPSS Inc., Chicago, USA). Spontaneous firing rates were obtained from recordings without electrical or acoustic stimulation. Unit CF's were visually determined using response maps (Figure 3). Sound driven and spontaneous firing rates were exported to Sigmaplot, which was used to generate graphs of RLFs (i.e., firing rate v. acoustic level).

Response type classification

Units were classified based on the PSTH shape of their response to CF tones at least 20 dB above threshold. In guinea pigs, AVCN neurons show three typical response patterns to suprathreshold tone bursts that can be visualized as PSTHs: (i) Primary-like / Primary-like with notch, (ii) Chopper and (iii) Onset (Winter and Palmer, 1990). In AVCN, Primary-like (PL) responses are thought to originate from spherical bushy cells; while Primary-like with notch (PLn) responses are characteristic of globular bushy cells (Smith and Rhode, 1987). As shown previously in the guinea pig, pyramidal cell responses in DCN typically fall into one of three temporal firing patterns: (i) Chopper (C), (ii) Buildup (B) / Pauser-Buildup (PB) , and (iii) Onset (O; Stabler et al., 1996).

Histology

The location of the stimulating electrode in the SP5 was verified post mortem. To mark the electrode tracks, the stimulating electrodes were dipped in Fluoro-Gold (2%, Sigma-Aldrich, USA), before being inserted into the brain. An electrical lesion was also made at the end of the experiment to verify the location of the tip of the stimulating electrode. At the end of each experiment, the animal was decapitated and the head was immersed in 4% paraformaldehyde for 48 hours, then the brain was removed and immersed in 4% paraformaldehyde for 24 hours. The brain was immersed in 20% sucrose solution overnight and then cryosectioned at 100 µm. Slices were stained with Neutral Red and examined under light and epifluorescence to view the mark of the electrical lesion and Fluoro-Gold marks from the stimulating probes.

Results

Recordings were obtained from 21 units in the AVCN and DCN in response to CF tones preceded by current stimulation and to CF tones alone. Of those, 9 were PL (Figure 4Bi), 6 were PLn units (Figure 4Bii), 2 were O (Figure 4Biii) units, 3 were PB units (Figure 4Biv), and 1 was classified as Unusual (Figure 4A).

The locations of the tips of the stimulating electrodes for all experiments in Sp5 are shown in Figure 2Bi. Reconstruction shows that the stimulating electrodes were located in either Sp5i or Sp5c, regions of the Sp5 from which projections to CN were observed (Zhou and Shore, 2004). DCN units were recorded from the dorsal channels of the recording probe; ventral channels of the same probe were located in the AVCN (Figure 2Biii).

Rate level functions (RLFs), which depict neural firing rate versus sound intensity, help to determine the threshold and dynamic range (range of sound levels over which firing rate changes with level). Changes in unit threshold and dynamic range after somatosensory stimulation will help to elucidate the function of the somatosensory-auditory neural circuits studied here.

Sp5 causes long-term excitation in AVCN neurons

In Figure 5A, firing rates from four RLFs conducted before bimodal stimulation were averaged and compared to the averaged firing rates from four RLFs recorded after bimodal stimulation. In this unit there was no significant difference in firing rate, between

the unimodal (tone alone; black graph in Figure 5A) and bimodal RLF (blue graph in Figure 5A), but in the 20 to 50 minutes following stimulation (red graph in Figure 5A) an increase can be observed. Like the unit in Figure 5A, 9 of 15 AVCN units from which recordings were conducted at CF, showed similar increases in firing rates after bimodal stimulation (Figure 6). Other units, though the acoustic stimulation was at CF, did not respond with persistent excitation or inhibition, demonstrating that the effect seen in units with long-term excitation was not due to a general increase in the excitability of the AVCN, but was specific for certain units in the AVCN and most likely dependent on their innervation by the somatosensory system.

Excitation in AVCN increases over time

While averaging firing rates from different RLF provides a general idea of the gross changes of firing rate, to examine the temporal course of the increase in firing rate after bimodal stimulation, Figure 5B plots the firing rates for one unit at four different times after bimodal stimulation had ceased. In this unit, while bimodal stimulation does not affect firing rate to the tones immediately, Figure 5B shows that firing rate at different acoustic stimulation levels above threshold increases over the 50 minutes time period during which recordings were conducted after bimodal stimulation. This trend was also evident across the total population of AVCN units. Figure 7 shows how across the population of AVCN neurons, acoustically driven firing rates measured 40 to 50 minutes after the bimodal stimulation show a higher driven rate than recordings conducted 20 – 30 minutes after bimodal stimulation.

Excitation in AVCN does not depend on cell type

The AVCN contains two principal types of bushy cells: spherical and globular, which correspond to PL and PLn acoustic responses. While having different morphologies and acoustic response properties (Hackney et. al., 1990; Winter and Palmer, 1990), both types of cells show a long term increase of firing rate after combined tone and current stimulation in SP5 (Figure 6). 7 out of 9 PL and 3 out of 6 PLn cells showed long-term increases in firing rate as described above and shown in Figure 5A. Both types of cells also have the same time course of rate increases after bimodal stimulation (Figure 7).

Sp5 causes long-term inhibition in DCN neurons

The same analysis was conducted for RLFs recorded from DCN units from the dorsal recording sites of the same electrode used to record AVCN units from more ventral sites (Figure 2Biii). In DCN, the opposite effect is seen compared to the AVCN. In Figure 8, firing rates from four RLFs conducted in a single unit before bimodal stimulation were averaged (black graph) and compared to the averaged firing rates from four RLFs conducted during (blue graph) and after bimodal stimulation (red graph). The averaged rates show a persistent suppression of firing rate during and after bimodal stimulation (Figure 8). This effect was consistent across the population of the 5 DCN units – both O and PB units (Figure 6). In DCN units, this effect also builds up over time with firing rate continuing to decrease over the 50 minutes following bimodal stimulation (Figure 7). However, while all DCN units showed persistent rate suppression after bimodal stimulation, only PB units showed a progressive decrease of firing rate over time while onset units did not (Figure 7). Instead, their firing rates decreased immediately after

12

bimodal stimulation, but showed no further decreases over the remainder of the recordings, which indicates that the somatosensory stimulation already reached its full effect at time 0. Even for the PB units the suppression seems to be faster developing compared to the excitation in AVCN units. This can also be seen for the example unit in Figure 8, which shows a maximum effect of the SP5 stimulation already during the stimulation.

Bimodal stimulation results in long-term changes of spontaneous rate

Spontaneous rates of firing were recorded during the course of the experiment at several times before and after bimodal stimulation. Figure 9 compares spontaneous rates before and approximately 10 minutes after bimodal stimulation in AVCN and DCN. 7 of 9 units that showed persistent enhancement in RLFs, also showed an increase in spontaneous rate by 5% to 54%; while 4 out of 5 units showing persistent inhibition demonstrated a decrease in spontaneous rate by 5% to 14% (Figure 9). Paired T-Tests comparing spontaneous rates from before Sp5 stimulation to spontaneous rates measured approximately 10 minutes after bimodal stimulation showed that there was a significant increase in spontaneous firing in AVCN, and a significant decrease in spontaneous firing in DCN ($p < 0.05$). For AVCN units, spontaneous rate recordings that were collected at least 30 minutes after Sp5 stimulation were compared to spontaneous rate recordings conducted approximately 10 minutes following bimodal stimulation (Figure 10). The spontaneous rate increased in 6 out of 7 units over the time lapse. Similar to acoustically evoked firing, spontaneous rates in AVCN showed a significant increase over time (Paired T-Test $p < 0.05$).

Discussion

<u>Persistent excitation seen in both PL and PL-N response types</u>

The AVCN contains two principal types of bushy cells: spherical and globular, which correspond to PL and PLn acoustic responses respectively (Smith and Rhode, 1987; Winter and Palmer, 1990). In addition, SBCs have an average spontaneous firing rate of approximately 59 spikes/sec that is higher than that of GBCs, which is, on average 12 spikes/sec (Smith et. al., 1993). There are also differences in morphology that may contribute to difference in acoustic response properties. Spherical bushy cells, as their name suggests, have a spherical cell body and one or two main dendrites that branch extensively creating a bushy appearance upon Nissl staining, while globular bushy cells have a more elongated soma and a less dense dendritic field (Hackney et. al., 1990). While these differences exist, both types of bushy cells respond with persistent excitation after bimodal stimulation suggesting that both types of bushy cells receive a similarly organized projection from Sp5. In addition to projections from Sp5 to the somata of putative bushy cells (Zhou and Shore, 2004), some of the Sp5 projections to the GCD, may terminate on to the dendrites of bushy cells that extend into the GCD (Gomez-Nieto and Rubio, 2009). Another possibility is that Sp5 projections to granule cells, in turn could project to bushy cells dendrites in the GCD. Nevertheless, these projections show no differentiation between SBCs and GBCs (Gomez-Nieto and Rubio, 2009) providing anatomical evidence to the finding that both types of AVCN cells show persistent excitation after bimodal stimulation.

Persistent inhibition in DCN

In contrast to AVCN, DCN neurons showed a persistent decrease in firing rate after bimodal stimulation. The cerebellar-like circuit of the DCN may provide an explanation for the inhibition of pyramidal cells (Figure 1). Glutamatergic Sp5 terminals activate granule cells in the GCD that sent an excitatory/glutamatergic projection (the parallel fibers) to pyramidal cells and cartwheel cells in the DCN. The latter sent an inhibitory (glycinergic) projection to pyramidal cells (Oertel and Young, 2004). The direct excitatory input from parallel fibers on pyramidal cells however, is usually weaker than the inhibitory input from cartwheel cells causing Sp5 stimulation to elicit primarily an inhibitory response in DCN during unimodal electric stimulation (Waller et al., 1996). This arrangement would predict that the long-term responses to bimodal stimulation on DCN pyramidal cells would be inhibition, assuming that the inhibition seen in unimodal responses directly leads to inhibition in the bimodal condition.

Synaptic plasticity might contribute to persistent response in AVCN and DCN

Bimodal stimulation leads to persistent changes in acoustically driven firing rate as well as spontaneous rates in AVCN and DCN. While the mechanisms underlying the interactions between the somatosensory and auditory systems remains to be fully elucidated, one possible explanation is that synaptic plasticity in the CN causing a change in the acoustic response properties of CN neurons is triggered through long-term depression (LTD) or long-term potentiation (LTP) that involves cartwheel and pyramidal cells in the DCN (Fujino and Oertel, 2003; Tzounopoulos et al., 2004) and perhaps bushy cells in the AVCN. In DCN, LTD and LTP have been shown to be

mediated by postsynaptic activation of a combination of different receptors, including both metabotropic glutamate and N-methyl-D-aspartate (NMDA) receptors at synapses between parallel fibers and fusiform and cartwheel cells (Petralia et al., 1996; Rubio and Wenthold, 1997; Fujino and Oertel, 2003) and presynaptic cannabinoid receptors (Zhao et. al., 2009). Release of post-synaptic intracellular Ca2+ has also been shown to be necessary for the generation of LTP/LTD (Fujino and Oertel, 2003; Nelson et. al. 2003). Circuit plasticity has been predicted through modeling to have an effect on how neurons respond to acoustic stimulation (Tzounopoulos, ARO 2010). Generation of LTP/LTD in local DCN circuits leads to more depolarized resting states of neurons, which then require less input before an action potential is fired, allowing for greater general excitability (Tzounopoulos, ARO 2010). Plasticity also leads to enlarged integration window over which excitatory inputs summate leading to greater rates of firing (Tzounopoulos, ARO 2010). The time course of the excitation and inhibition that is seen also correlates with LTP/LTD responses. LTP/LTD are long-term responses lasting minutes after the initial stimulation, much like the prolonged excitation and inhibition that is seen after bimodal stimulation. In DCN, if the synapse between parallel fibers and cartwheel cells was plastic, cartwheel cells would consequently send greater inhibitory input to pyramidal cells. Plasticity as an explanation for prolonged excitation in AVCN also suggests that Sp5 input to AVCN could be indirect through the granule cells. Investigation using analysis of latencies of response of AVCN neurons to unimodal Sp5 stimulation would be a further line of investigation in order to determine if the inputs from Sp5 are direct or indirect.

While long-term changes in AVCN after somatosensory stimulation have not been previously observed, long term inhibition of DCN spontaneous rates after electrical stimulation can occur (Zhang and Guan, 2008). An important finding of Zhang and Guan (2008) was that suppression of spontaneous rate was dependent on the intensity of the electrical stimulation. In this study, the intensity of Sp5 stimulation was not varied. Future study could involve observing if there is a change in acoustically driven rate based on different intensities of electrical stimulation.

Results here indicate that somatosensory input has significant effect on the long-term responses of both DCN and AVCN neurons, which may be attributed to synaptic plasticity in local CN circuits. Changes in the CN circuits are important because of the impact on the response of higher order neurons that receive projections from the CN. Somatosensory inputs into the CN have previously been speculated to have different functions such as suppression of self-generated noise, sound localization and have been studied as possible physiological correlates of somatic tinnitus (Haenggeli et. al., 2005, Kanold and Young, 2001; Bell et al., 1997; Shore, 2005). Given the results of this study, perhaps plasticity changes are also a part of these processes.

References

Bell C. Bodznick D, Montgomery J, Bastian J.1997. The generation and subtraction of sensory expectations within cerebellum-like structures. Brain Behav Evol 50:17-31.

Cant NB, Benson CG. 2003. Parallel auditory pathways: projection patterns of the different neuronal populations in the dorsal and ventral cochlear nuclei. Brain Res Bull. 60(5-6):457-74.

Capra NF. 1987. Localization and central projections of primary afferent neurons that innervate the temporomandibular joint in cats. Somatosens Res 4:201–213.

Fujino K, Oertel D. 2003. Bidirectional synaptic plasticity in the cerebellum-like mammalian dorsal cochlear nucleus. Proc Natl Acad Sci USA 100:265–270.

Gómez-Nieto R, Rubio ME. 2009. A Bushy Cell Network in the Rat Ventral Cochlear Nucleus. J Comp Neurol 516:241-263.

Hackney, C.M., Osen, K.K. & Kolston, J. (1990) Anatomy of the cochlear nuclear complex of guinea pig. Anat. Embryol. (Berl.) 182:123–149.

Haenggeli CA, Pongstaporn T, Doucet JR, Ryugo DK. 2005. Projections from the spinal trigeminal nucleus to the cochlear nucleus in the rat. J Comp Neurol 484(2):191-205.

Jacquin MF, Barcia M, Rhoades RW. 1989. Structure-function relationships in rat brainstem subnucleus interpolaris: IV. Projection neurons. J Comp Neurol 282:45–62.

Kanold PO, Young ED. 2001. Proprioceptive information from the pinna provides somatosensory input to cat dorsal cochlear nucleus. J Neurosci 21:7848-7858.

Kirzinger A, Jurgens U. 1991. Vocalization-correlated single-unit activity in the brain stem of the squirrel monkey. Exp Brain Res 84:545-560.

Luthe L, Hausler U, Jurgens U. 2000. Neuronal activity in the medulla oblongata during vocalization. A single-unit recording study in the squirrel monkey. Behav Brain Res 116(2):197-210.

Nazruddin, Suemune S, Shirana Y, Yamauchi K, Shigenaga Y. 1989. The cells of origin of the hypoglossal afferent nerves and central projections in the cat. Brain Res 490:219 –235.

Nelson AB, Krispel CM, Sekirnjak C, du Lac S. 2003. Long-lasting increases in intrinsic excitability triggered by inhibition. Neuron 40:609-620.

Oertel D, Young ED. 2004. What's a cerebellar circuit doing in the auditory system? Trends Neurosci 27(2):104-110.

Petralia RS, Wang YX, Zhao HM, Wenthold RJ. 1996. Ionotropic and metbotropic glutamate receptors show unique postsynaptic, presynaptic, and glial localizations in the dorsal cochlear nucleus. J Comp Neurol 372:356–383.

Romfh JH, Capra NF, Gatipon GB. 1979. Trigeminal nerve and temporomandibular joint of the cat: a horseradish peroxidase study. Exp Neurol 65:99–106.

Rubio ME, Wenthold RJ. 1997. Glutamate receptors are selectively targeted to postsynaptic sites in neurons. Neuron 18:939–950.

Ryugo DK, Haenggeli CA, Doucet JR. 2003. Multimodal inputs to the granule cell domain of the cochlear nucleus. Exp Brain Res 153(4):477-85.

Shore SE, Vass Z, Wys NL, Altschuler RA. 2000. Trigeminal ganglion innervates the auditory brainstem. J Comp Neurol 419:271–285.

Shore SE, El-Kashlan HK, Lu J. 2003. Effects of trigeminal ganglion stimulation on unit activity of ventral cochlear nucleus neurons. Neuroscience 119:1085–1101.

Shore SE. 2005. Multisensory integration in the dorsal cochlear nucleus: unit responses to acoustic and trigeminal ganglion stimulation. Eur J Neurosci 21(12):3334-3348.

Shore SE, Koehler S, Oldakowski M, Hughes LF, Syed S. 2008. Dorsal cochlear nucleus responses to somatosensory stimulation are enhanced after noise-induced hearing loss. Eur J Neurosci 27(1):155-168.

Stabler SE, Palmer AR, Winter IM. 1996. Temporal and mean rate discharge patterns of single units in the dorsal cochlear nucleus of the anesthetized guinea pig. J Neurophysiol 76(3):1667-1688.

Suemune S, Nishimori T, Hosoi M, Suzuki Y, Tsuru H, Kawata T, Yamauchi K, Maeda N. 1992. Trigeminal nerve endings of lingual mucosa and musculature of the rat. Brain Res 586:162–165.

Smith PH, Phillip JX, Yin T. 1993. Projections of Physiologically Characterized Spherical Bushy Axons From the Cochlear Nucleus of the Cat: Evidence for Delay Lines to the Medial Superior Olive. J. Comp. Neurol

Takemura M, Sugimoto T, Shigenaga Y. 1991. Difference in central projection of primary afferents innervating facial and intraoral structures in the rat. Exp Neurol 111:324–331.

Tzounopoulos T, Kim Y, Oertel D, Trussell LO. 2004. Cell-specific, spike timing-dependent plasticities in the dorsal cochlear nucleus. Nat Neurosci 7(7):719-725.

Tzounopoulos T. 2010, "Dynamic Range Adaptation by Coordinated LTP and LTD", Association for Reasearch in Otolarygnology, Anaheim, CA.

Waller HJ, Godfrey DA, Chen K. 1996. Effects of parallel fiber stimulation on neurons of rat dorsal cochlear nucleus. Hear Res 98:169–179.

Weinberg RJ, Rustioni A. 1987. A cuneocochlear pathway in the rat. Neuroscience 20:209–219.

Winter IM, Palmer AR. 1990. Responses of single units in the anteroventral cochlear nucleus of the guinea pig. Hear Res 44:161-178.

Wright DD, Ryugo DK. 1996. Mossy fiber projections from the cuneate nucleus to the dorsal cochlear nucleus. J Comp Neurol, 365:159–172.

Zhang J, Guan Z. 2008. Modulatory effects of Somatosensory electrical stimulation on neural activity of the dorsal cochlear nucleus of hamsters. J Neurosci Res 86:1178–1187.

Zhou J, Nannapaneni N, Shore S. 2007. Vessicular glutamate transporters 1 and 2 are differentially associated with auditory nerve and spinal trigeminal inputs to the cochlear nucleus. J Comp Neurol 500(4):777-787.

Zhou J, Shore S. 2004. Projections from the trigeminal nuclear complex to the cochlear nuclei: A retrograde and anterograde tracing study in the guinea pig. J Neurosci Res 78(6):901-907.

Zhao Y, Rubio ME, Tzounopoulos T. 2009. Distinct functional and anatomical architecture of the endocannabinoid system in the auditory brainstem. J Neurophysiol 101(5):2434-46.

Figures

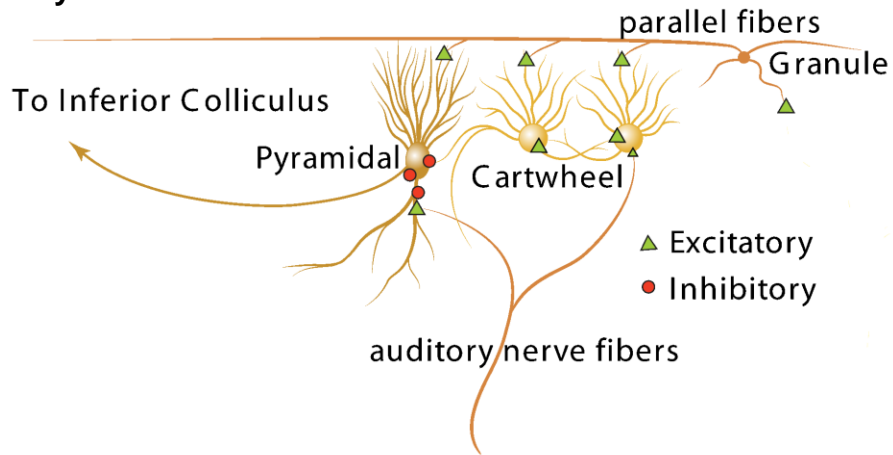**Figure 1: Schematic illustrating known anatomical and physiological components of DCN circuitry.**

Figure 2: Specifics of Recording and Stimulating Probe

A. Dimensions of 16-channel single-shank recording (picture from NeuroNexus Technologies, March 2008). (i) Dependent on the experiment, between 2 to 3 mm of the probe were inserted into the brain. (ii) Site map showing the location of channels of the probe, which are spaced 100 μm apart. Channel 6, the ventral most channel, is located 50 μm from the tip of the probe.

i.
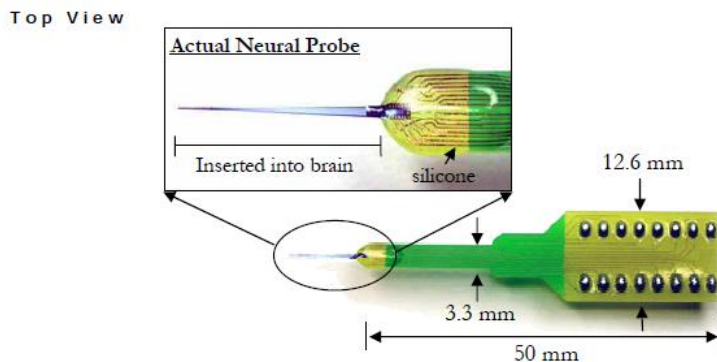
ii.
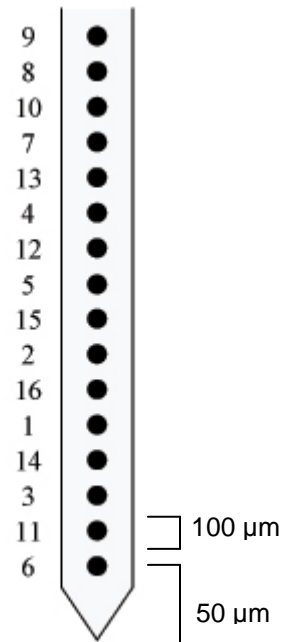
B. Sp5 Electrode Positions

(i) Positions of tip of Sp5 stimulation electrode from post-mortem reconstructions of the electrical lesions are indicated. In all experiments, the electrode was located in the Sp5i or Sp5c, regions from which projections to CN have been shown. sp5=spinal trigeminal tract, Sp5I/Sp5C=intermediate/caudal subdivision of Sp5, Cu=cuneate nucleus, Gr=gracile nucleus (ii) Stained transverse section of brainstem visualized under UV. The fluorescent marker shows that the tip of the stimulating electrode is located in Sp5i. (iii) Site map of recording electrode showing the location of channels recording in DCN and AVCN. Channels which recorded DCN unit types were more dorsal consistent with CN anatomy.

i.
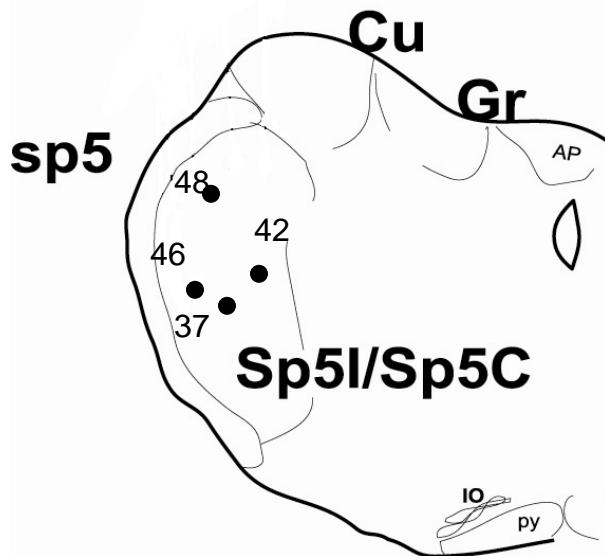
iii.
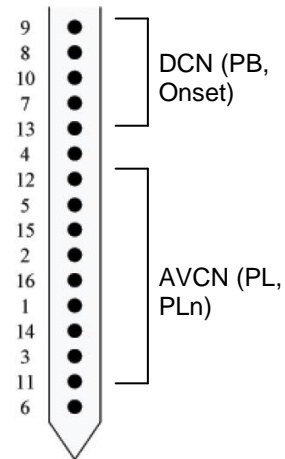
ii.
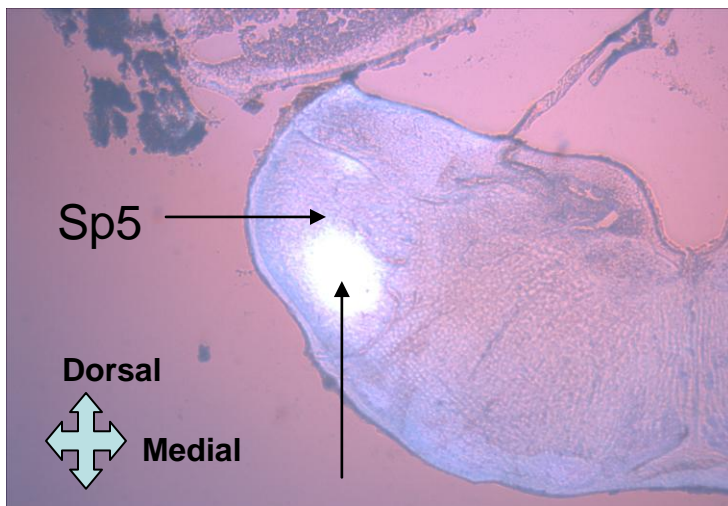
Figure 3: **Response Map used to determine characteristic frequency**
Response map shows the PSTHs of responses to acoustic stimulation for every frequency/level combination for 2982 – 23856 Hz (incrementing by 0.1 octave steps) and 0 – 85 dB (incrementing by 5 dB steps at every frequency). Comparing across multiple frequencies, 14683 Hz is the center of the V-shaped response curve (see green arrows) that stretches from approximately 6000 Hz to 24000 Hz and therefore was judged to be the characteristic frequency of the unit.
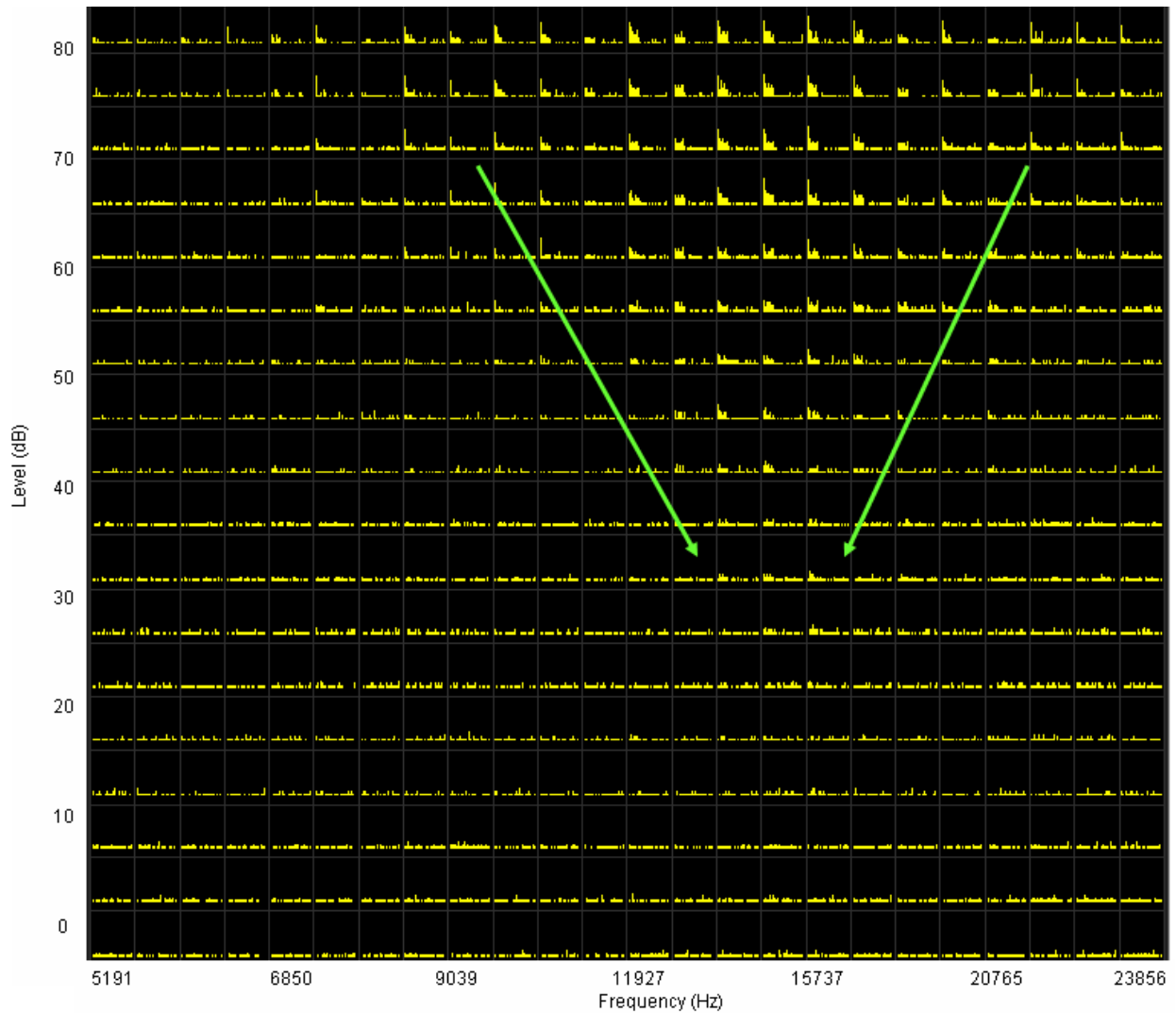
Figure 4: **Major acoustic response types recorded from in AVCN and DCN.**
A. Percent of units falling into each class: 9/21 PL, 6/21 PLn, 2/21 O, 3/21 PB and 1/21 U. B. Acoustic responses at CF were recorded at 20 dB above threshold for 300 repetitions to generate PSTHs. Cells in AVCN and DCN have specific acoustic response types that were used for unit classification. These are: (i) Primary-like (PL) acoustic response, that originates from the Spherical Bushy Cells in the AVCN, (ii) Primary-like with Notch (PLn) acoustic response from Globular Bushy cells in the AVCN, (iii) Onset response and (iv) Pauser-Buildup response from DCN pyramidal cells.

A.

B.

23
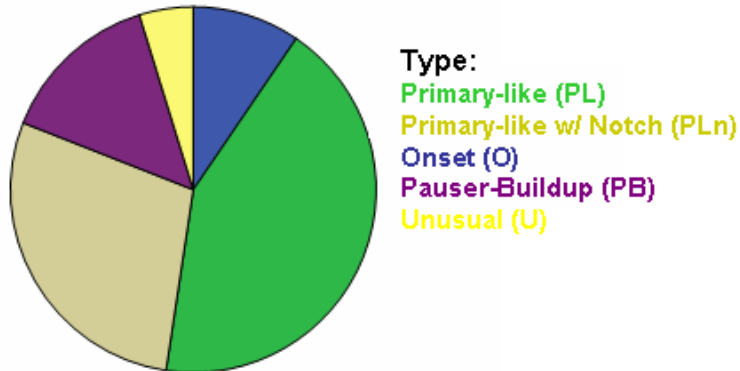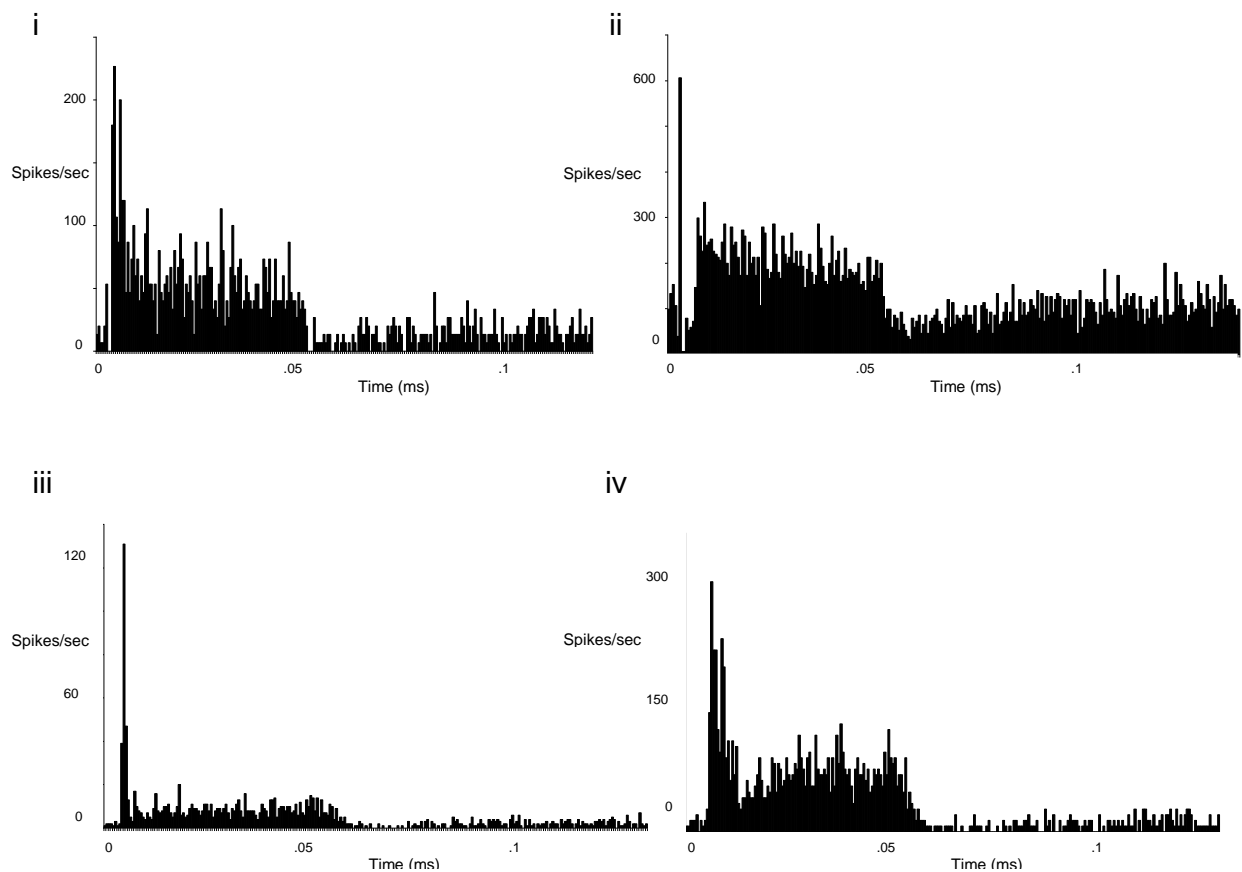
Figure 5: **Persistent increase in firing rate in AVCN neurons**
   A. Averaged CF-tone RLFs for one multiunit channel before (N=4 RLFs), during
      (N=1 RLF) and 20-50 minutes after bimodal stimulation (N=4 RLFs). The unit
      was classified as Primary-like and was therefore presumed to be from one or
      more SBCs in the AVCN (inset shows PSTH recorded at 20 dB above
      threshold that was used for response typing). An increase in firing rate to the
      tone is seen across all levels after bimodal stimulation (red). Error bars show
      standard deviation from the averaging of RLFs. In this unit, bimodal
      stimulation (blue) does not create a change in firing rate that can be seen
      immediately during the bimodal stimulation.
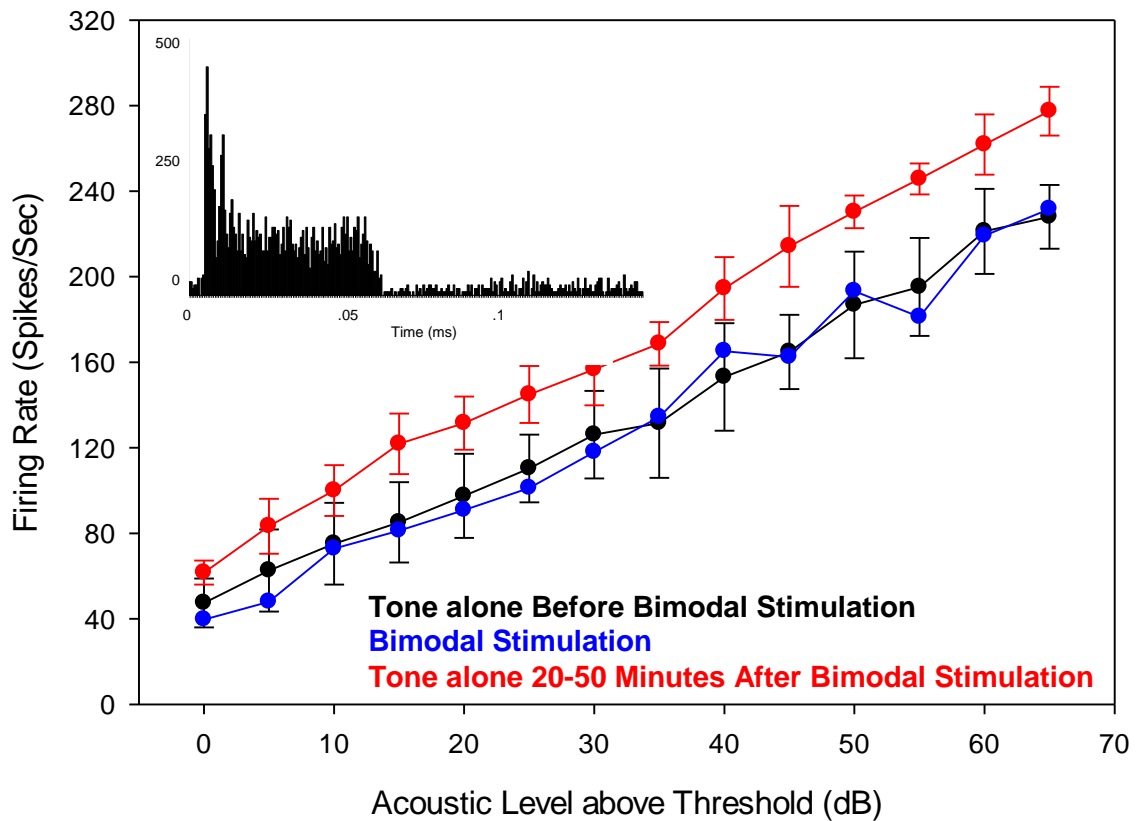
B. In the same unit, progressive increases in firing rate over time can be seen. Spike rates recorded at specific times after bimodal stimulation (Time = 0) are shown for each level. The data point at -1 is an average of firing rates from before bimodal stimulation. The following data points are from single RLFs conducted at different times after bimodal stimulation. After bimodal stimulation, a gradual increase in firing rate can be observed over the 45 minute time span during which recordings were conducted.
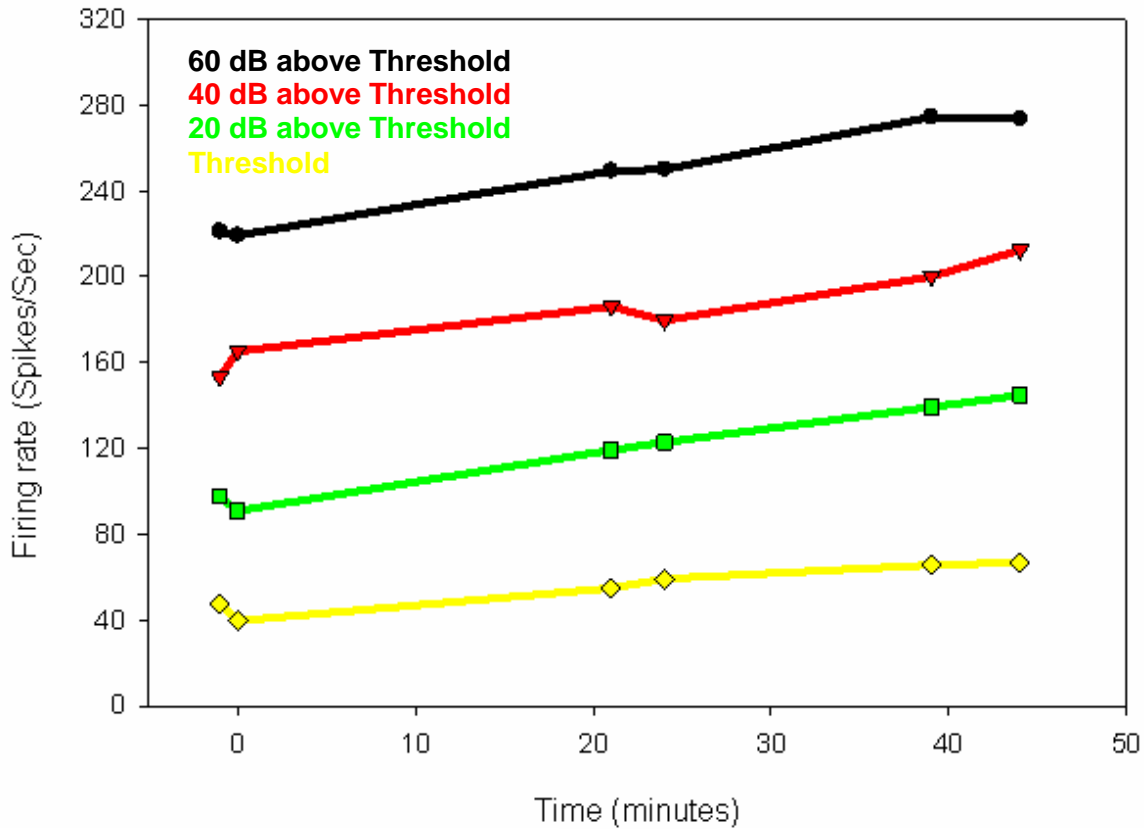
Figure 6: **Firing rates to acoustic stimulation change after Sp5 Stimulation**
For all units showing a long-term response to bimodal stimulation (n= 14/21 units), the difference between averaged spike rates from before (4 RLFS) and after bimodal stimulation (4 RLFs) was calculated for every level from 5 – 85 dB. The graph shows that PL and PLn units in the AVCN (blue; n=9 units with PL/PLN responses) increase their spike rate after bimodal stimulation as shown by spike rates above the zero line, whereas DCN units (green and red; n=3 units with PB responses; n=2 units with O responses) have a decrease in firing rate after Sp5 stimulation (rates below the zero line).
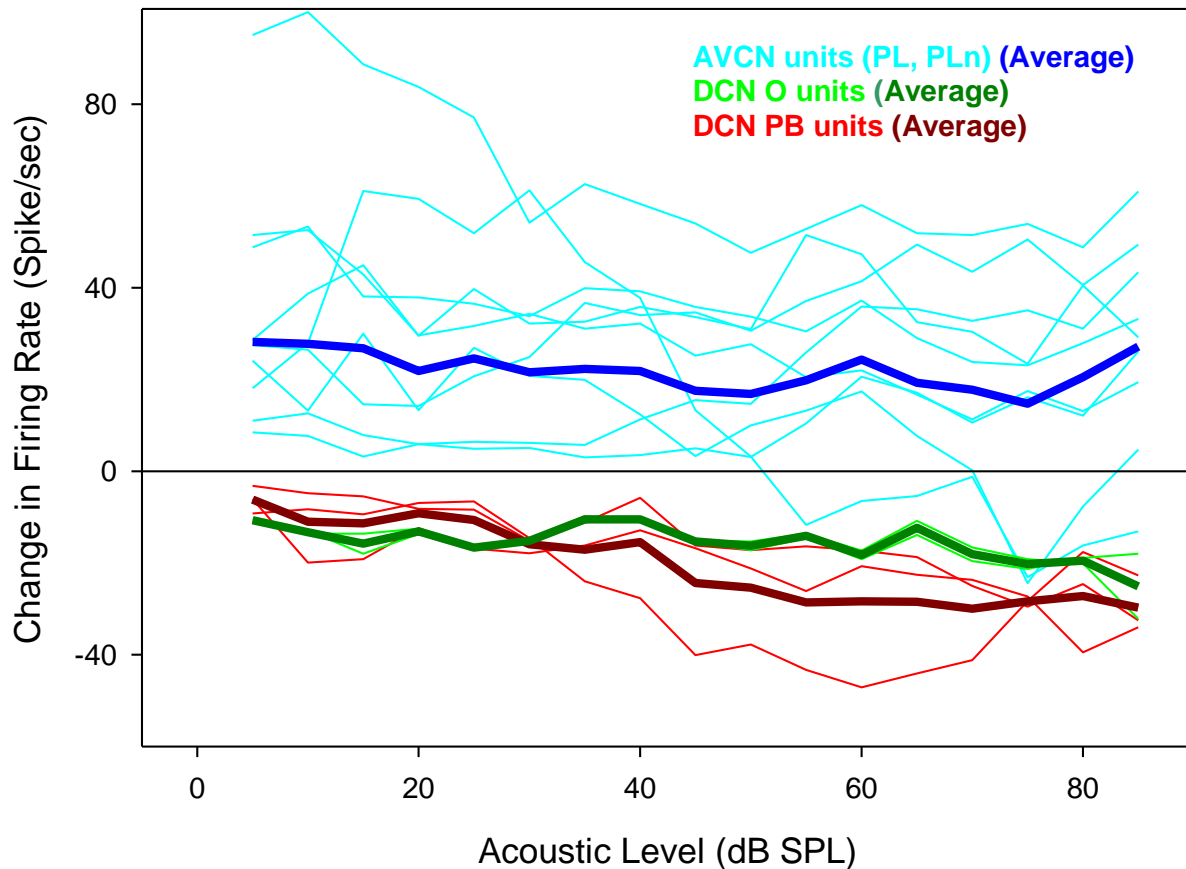
Figure 7: **Firing rates to acoustic stimulation after bimodal stimulation accumulate over time**

To determine how firing rates of each unit changes over time, in those units showing a long-term response after bimodal stimulation, the firing rates after bimodal Sp5 stimulation were normalized to the average firing rates before bimodal stimulation. Shown here are the firing rates at 40 dB above threshold. PL and PLn AVCN units showed an increase in firing rate over time. PB units in DCN showed a clear decrease in firing rate over time, while onset units showed a decrease in overall firing rate, but did not decrease in firing rate over time.
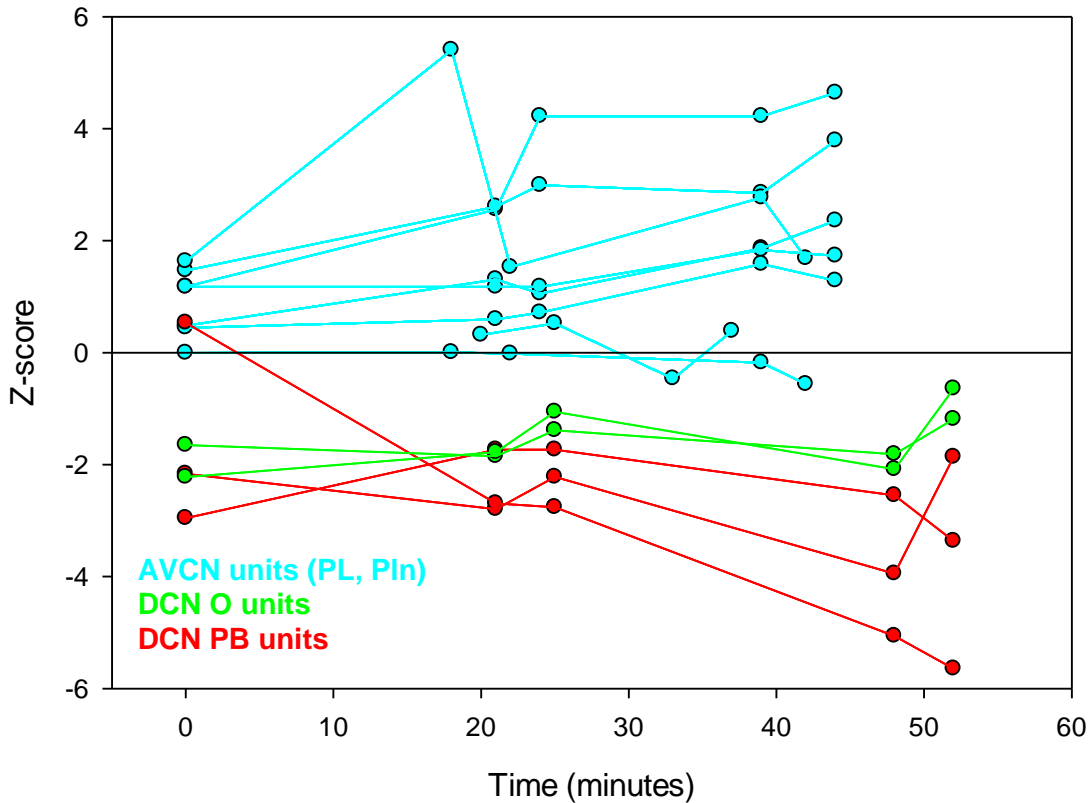
Figure 8: **Persistent decrease in firing rate in DCN**

A. Averaged CF-tone RLFs for one single unit channel before (N=4 RLFs), during (N=1 RLF) and 20-50 minutes after bimodal stimulation (N=4 RLFs). The unit was classified as Pauser-Buildup and is therefore a pyramidal cell in the DCN (inset shows PSTH recorded at 20 dB above threshold that was used for response typing). A decrease in firing rate to the tone is seen across all levels during (blue) and after bimodal stimulation (red). Error bars show standard deviation from the mean of RLFs.
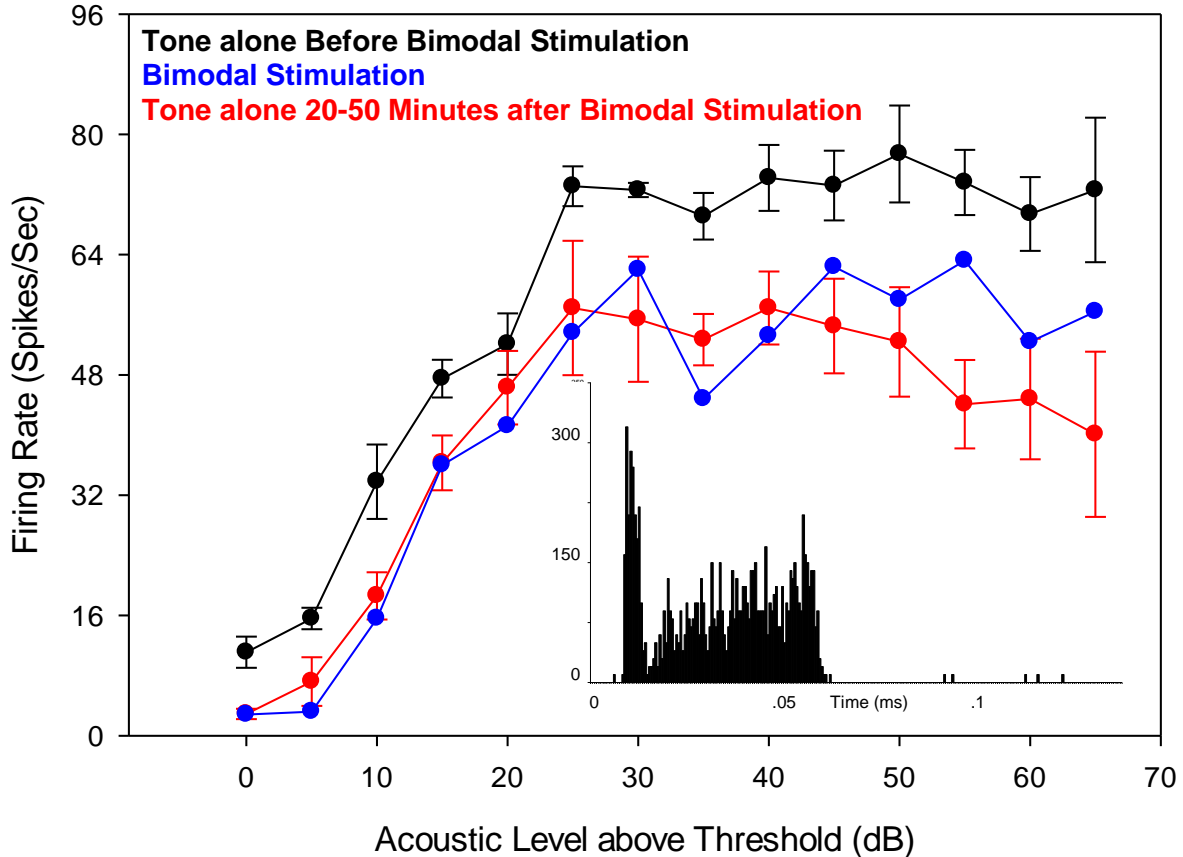
Figure 9: **Bimodal stimulation leads to long-term changes spontaneous rates**
Comparison of spontaneous rates before and approximately 10 minutes after bimodal stimulation. Units showing an increase will be above the reference line of x=1, while decreases will be located below. Units were grouped by location in CN. 7 out of 9 AVCN units showed increased spontaneous rate after bimodal stimulation (5% - 54%), while 4 out of 5 DCN units showed a decrease (5% - 14%).
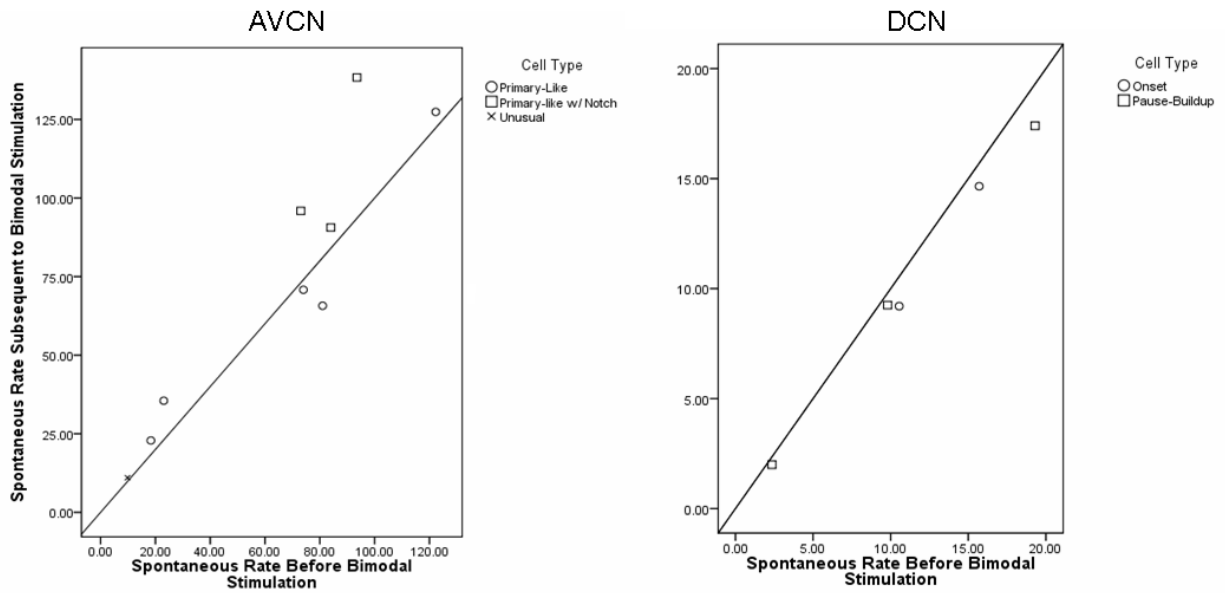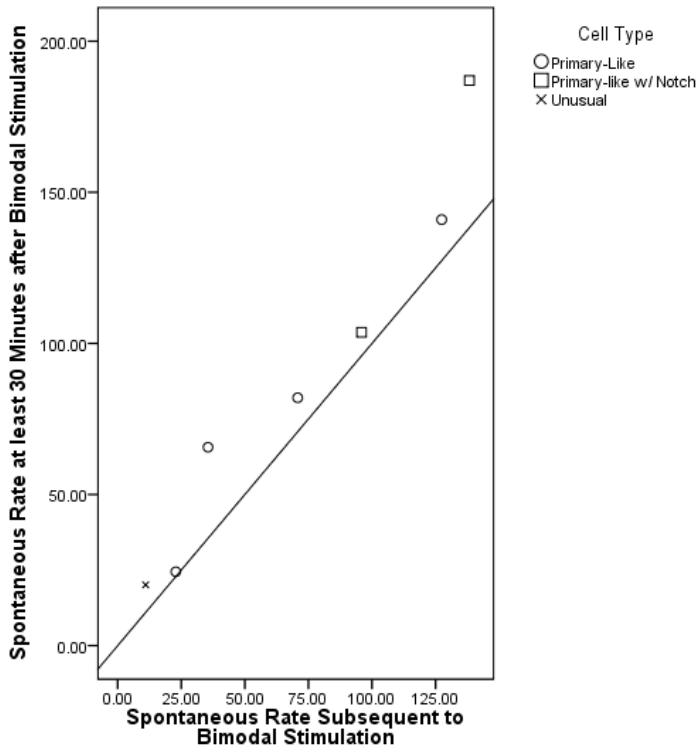
Figure 10: **Spontaneous rate changes accumulate over time**
> Comparison of Spontaneous rates of firing approximately 10 minutes after and at least 30 minutes after Sp5 stimulation show an increase in firing rate over the time interval. 6 out of 7 data points are above the x=1 line indicating an increase in the rate of firing. Data points are only available for AVCN units, so conclusions cannot be made about DCN units. The data also suggests that at least for AVCN units spontaneous rates are increasing over time, like sound driven rates.

Acknowledgements